JOURNAL OF GEOPHYSICAL RESEARCH, VOL. 85, NO. C3, PAGES 1621-1632, MARCH 20, 1980

Simultaneous Spectroscopic Measurements of Stratospheric Species: O_3, CH_4, CO, CO_2, N_2O, H_2O, HCl, and HF at Northern and Southern Mid-Latitudes

C. B. FARMER

Division of Geological and Planetary Sciences, California Institute of Technology, Pasadena, California 91125

O. F. RAPER, B. D. ROBBINS, AND R. A. TOTH

Jet Propulsion Laboratory, California Institute of Technology, Pasadena, California 91103

C. MULLER

Institute d'Aeronomie, Brussels, Belgium

Near-infrared solar absorption spectra have been recorded in the course of balloon flights from Palestine, Texas, (32°N latitude) in May 1976, and Broken Hill, Australia, (30°S latitude) in March 1977. The northern flight was made at a float altitude of 37 km and covered the spectral region from 1800 cm^{-1} to 3600 cm^{-1}, which encompasses infrared transitions of O_3, CH_4, CO, CO_2, N_2O, H_2O, and HCl. The flight in the southern hemisphere, from a float altitude of 39 km, covered the spectral region from 2800 cm^{-1} to 4500 cm^{-1}, which includes useful transitions for all of the above gases (with the exception of CO) and encompasses as well the 1-0 fundamental band for HF. Both sets of spectra were acquired at sunset by using a high-resolution (0.13 cm^{-1}) Michelson interferometer. The simultaneous profiles of concentration derived from the spectra for the individual gases covered in each flight are presented and discussed. While the results show few differences between the profiles at the northern and southern latitudes, there are several aspects of general importance; these include lower values for stratospheric CO than had previously been reported (i.e., ~10 ppbv), and water vapor profiles in both hemispheres showing an increase with altitude considerably in excess of that to be expected from CH_4 oxidation alone. The shape of the profile for HF was found to be consistent with model predictions, but the HF concentrations were lower by a factor of 3 or 4 than those predicted.

INTRODUCTION

The present decade has seen greatly increased efforts in all aspects of upper atmospheric research in response to the growing awareness of the need to understand more thoroughly the chemical and dynamical processes which control the stability of the atmosphere. The initial emphasis in measurements has been to establish the presence in the stratosphere of particular trace molecular species and, where possible, to obtain concentration profiles. The species chosen were those which were felt to be of prime importance in gaining insight into the processes which control the stability of the stratospheric compositional inventory as a whole. This approach was the natural response of experimentalists in their initial attempts to use existing techniques to provide pertinent data as quickly as possible to aid atmospheric chemists and modelers in the assessment of potentially crucial problems. The rapid growth of activity in the theoretical field has also resulted in the development of a large number of models of varying degrees of sophistication which provide the methodology essential to the understanding and objective evaluation of potential disturbances to this stability.

An important outcome of the progress made with these studies of the mechanisms controlling the upper atmosphere is the realization that simultaneous measurements of groups of constituents are much more useful as input to the models than are isolated measurements of individual species. This is true even for the more familiar 'natural' trace molecules, as a consequence of the highly interactive nature of the problem. Thus the current thrust in measurements programs designed to support the more realistic use of theoretical models is to obtain simultaneous data on the distributions of selected groups of molecules to constrain the models to the point where acceptable accuracy in model predictions can be achieved.

For the past several years we have been engaged in a research program designed to study the composition of the earth's atmosphere and its seasonal and geographic variability. The measurements have been made from the ground and from a variety of airborne platforms (i.e., medium- and high-altitude aircraft and balloons), using a high-resolution Fourier interferometer operating in the 1.3- to 5.5-μm wavelength region of the infrared. Most polar molecules have transitions that occur in this wavelength region, and thus a single spectrum contains useful information for a large number of atmospheric species. The spectra are normally recorded in absorption, using the sun as the radiation source and the geometry of sunrise or sunset observation to provide the advantages of long atmospheric paths and the necessary weighting functions for the derivation of vertical concentration profiles [*Farmer*, 1974]. The usual procedure from airborne platforms is to generate interferograms continuously over the range of solar zenith angles from 90° to 95°; each complete interferogram is generated in ~100 s, which corresponds to a height resolution of between 1 and 4 km, depending on the solar zenith angle and the altitude of the observation platform. After the data are transformed the resultant spectra are used to establish either the presence of, or useful upper limits for, a number of trace species, and to deduce vertical distributions for those

Paper number 9C1593.
0148-0227/80/009C-1593$01.00

constituents which are present in sufficient concentrations to provide measurable features in successive spectra.

This report covers the results of two balloon flights. The first was made from Palestine, Texas, in the spring of 1976, during which concentration profiles for O_3, CO, CO_2, CH_4, N_2O, H_2O, and HCl were obtained. The second flight was made in the late summer of 1977 from Broken Hill, Australia, and produced data on the vertical distributions of O_3, CO_2, CH_4, N_2O, H_2O, HCl, and HF. The spectral features used for analysis and the estimated errors are discussed below for the individual molecules in each data set.

EXPERIMENTAL

The observations were made with a modified Connes-type Michelson interferometer which utilizes cat's-eye retroreflectors in both the fixed and moving arms. An earlier version of the instrument was described by *Schindler* [1970]. A number of modifications and additions to the original system have been made for the present flights resulting in significant improvements to its operation and performance, and a brief description of its current configuration will be given. Radiation from a sun tracker is divided at the beamsplitter, passes through each cat's-eye to a fixed retro mirror, and is then reflected back to the beamsplitter along the same optical path. The moving cat's-eye is 'stepped' between sample points under the control of a He · Ne laser, the optical path difference being held constant while each sample point is acquired. Stepping is accomplished by controlling the position of the low-inertia secondary mirror, which is mounted on a piezoelectric stack in the moving cat's-eye. During each sample period the radiation is modulated internally by applying a 8 kHz signal to this same piezoelectric stack.

The optical configuration and sampling method used in the instrument have several performance advantages over those used in the more conventional single-pass continuous-drive systems, particularly with regard to insensitivity to thermally or mechanically induced misalignments and the control which a digital system permits in the aggregation of complete interferograms. Double-passing the radiation through the cat's-eyes renders the instrument insensitive to small tilts or shears in the critical optical components and also doubles the optical path retardation of the interferometer and hence its spectral resolution. The advantages in an adverse environment of incrementing the optical path in discrete steps and locking it under servocontrol during sampling are obvious; an additional advantage is gained by driving the servo system with an up-down fringe counter and comparator which prevents it from skipping any sample points in the event of temporary loss of lock.

The limits to the wavelength coverage of the instrument during these flights were 1.3 μm (7900 cm^{-1}) and 5.5 μm (1800 cm^{-1}), set by the aliasing requirement of the reference laser, and the long wavelength cutoff of the detector (InSb at liquid nitrogen temperature), respectively. The instrument was capable of covering this entire wavelength region in 200 s. However, to improve the spatial resolution and to simultaneously preserve the full spectral resolution, order isolation filters were used during both flights. For the Texas flight the spectral limits set by the filter were 1800 cm^{-1} and 3600 cm^{-1}; for the Australian flight the decision was made to operate with a filter covering the 2880-cm^{-1} to 4550-cm^{-1} region to include the 1-0 HF band at 4000 cm^{-1}.

In the balloon configuration the instrument optical head and sun tracker were mounted in the gondola together with the control and data handling subsystems, a backup analog tape recorder, and the telemetry and command interface units. In flight the azimuthal orientation of the gondola was monitored by telemetry from an onboard magnetometer and controlled by a torque motor and reaction bar. During data-taking sequences this inertial control system was slaved to a gondola sun sensor which kept the gondola correctly oriented to the sun to within ±2°. The instrument field-of-view pointing vector was controlled in both azimuth and elevation to ±1 min of arc by the solar tracker. The tracker, designed and built by Ball Brothers Research Corporation specifically for use with the interferometer, is coupled to the instrument's servocontrol system and automatically inhibits the stepping process if the tracker loses solar lock as a result of any sudden change in gondola orientation. The total gondola weight, including batteries and ballast, was approximately 900 kg.

The flight from Palestine was launched on the afternoon of May 18, 1976, reaching a float altitude of 37 km. At sunset the balloon and gondola were about 50 n. mi. (93 km) due west of the launch site (at 31.8°N latitude, 96.7°W longitude). Several low air mass interferograms were recorded prior to sunset on this flight and 10 during sunset at solar elevation angles from 0.20° to −4.48°. The Broken Hill flight was launched at dawn on March 23, 1977, and reached its float altitude of 39 km 2 hours later. During ascent, 20 spectra were recorded at balloon altitudes from 15 to 39 km and solar elevation angles from 9.4° to 24.8°. By sunset the balloon had floated some 240 n. mi. (444 km) southwest of Broken Hill (to 30.4°S, 138.7°E). Prior to sunset, an additional 20 spectra were recorded (including the use of a germanium filter which covered the wavelength region from 1800 to 6000 cm^{-1}) at solar elevation angles between 14.6° and 0.6°. At sunset, 18 spectra were recorded at solar elevation angles from 0° to −6°. During the night the winds aloft carried the payload out of telemetry range, and thus a planned sunrise transition could not be acquired.

ANALYSIS OF THE SPECTRA

The molecular vibration-rotation bands used for the analysis are given in Table 1 for each of the species covered in the

TABLE 1. Observed Vibration-Rotation Bands for the Species Covered in the Flights

Molecule	Band	Central Frequency, cm^{-1}
CO	1–0	2147
N_2O	ν_3	2224
CO_2	ν_3	2349
N_2O	$\nu_1 + 2\nu_3$	2462
N_2O	$2\nu_1$	2564
CH_4	$2\nu_4$	2600
CO_2	$2\nu_1$	2614
O_3	$\nu_1 + \nu_2 + \nu_3$	2785
CH_4	$\nu_2 + \nu_4$	2823
HCl	1–0	2905
CH_4	ν_3	3019
O_3	$3\nu_3$	3041
H_2O	$2\nu_2$	3152
CO_2	$2\nu_1 + \nu_2$	3182
CO_2	$2\nu_1 + \nu_2$	3340
N_2O	$\nu_1 + \nu_3$	3481
CO_2	$\nu_1 + \nu_3$	3528
CO_2	$\nu_1 + \nu_3$	3612
HF	1–0	4005

flights. Except where indicated in the text, the relevant molecular parameters used for the individual analyses were taken from the *McClatchey et al.*, [1973] compilation. As will be seen from the following paragraphs dealing with the individual molecules, a considerable amount of laboratory work was necessary before the analysis could proceed to improve or extend the basic molecular spectroscopic data.

For most of the molecules reported on here, the data were analyzed in two stages. A preliminary concentration profile was first established, using the measured equivalent widths. This distribution was then used with a layered model atmosphere (1-km layer thickness) to generate synthetic spectra with the same viewing geometries as the observed spectra. The synthetic spectra were generated, utilizing standard line-by-line computational routines for the combined Lorentz-Doppler region appropriate to each atmospheric layer and convolved with the instrument function. The model profile was then modified in an iterative fashion until the differences between the real and synthetic spectra were minimized. Examples of the comparison between the final synthetic spectra generated with the model profile and the corresponding observed spectra are shown in the relevant sections below.

RESULTS

The two sets of vertical mixing profiles determined from this work are shown in Figures 1 and 2 and, for convenience, are listed in tabular form (Table 2), together with the atmospheric model used for the analyses; the individual distributions are compared and discussed in the paragraphs below. In the interest of preserving clarity the estimated errors for the individual species are not included in the figures but are discussed in their respective paragraphs. In most instances the final results for the concentration profiles shown here are in reasonable agreement with the values which have appeared in the recent literature, based on measurements involving similar spectroscopic techniques as well as in situ measurements. While no attempt has been made here to give an exhaustive comparison with the results of other workers, the degree of agreement or disagreement between these and previous results for each species is indicated.

Ozone

Although all of the O_3 fundamental bands occur at longer wavelengths than the regions covered by the present data, there are several overtone and combination bands which appear in the 2000- to 3000-cm^{-1} region of the stratospheric spectrum. In particular, in the Palestine spectra the $\nu_1 + \nu_2 + \nu_3$ band (centered at 2785.74 cm^{-1}) gives rise to a number of lines or groups of lines in the spectra whose intensities are ideally suited to the derivation of the O_3 profile. This band was not covered in the Australian spectra, but a number of lines from the $3\nu_3$ band centered at 3041.2 cm^{-1} were available for the analysis. Although the analysis was more difficult with the $3\nu_3$ lines, this band was common to both sets of spectra, and thus it was possible to correlate the two sets by using the $3\nu_3$ band and the $\nu_1 + \nu_2 + \nu_3$ band in the Palestine spectra and improve the relative accuracy of the measurements. Figures 3 and 4 show plots of the wavelength intervals encompassing these bands for several of the stratospheric spectra obtained during the flights. Those features which are marked with vertical lines in the figures were used for the derivation of the ozone distributions shown in Figures 1 and 2. The absolute accuracy of the O_3 concentration values is limited by uncertainty in the knowledge of the O_3 line strengths in these bands, the overall accuracy of the measurements in each case being estimated to be ±25%. It should be noted that while this uncertainty affects the total ozone burden, the shape of its distribution is essentially unaffected. As the figures illustrate, the two profiles are similar in shape, although the peak in the O_3 distribution occurs at a somewhat lower altitude in the Australian measurement (see Table 2).

There have been no previous infrared absorption measurements of the distribution of stratospheric ozone reported in the literature with which the present results can be compared; however, bearing in mind the differences in spatial averaging between the optical and in situ methods, and the expected variability of O_3, the present results are reasonable with regard to both the magnitude and the distribution of the stratospheric ozone layer. The real value of these results is the fact that they simultaneously represent the ozone profiles in con-

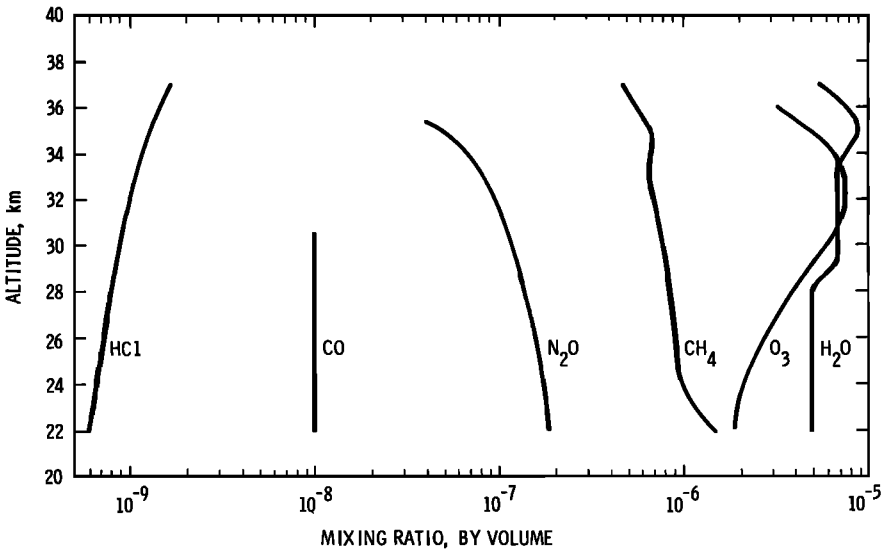

Fig. 1. Volume mixing ratios as a function of altitude for the minor and trace species indicated derived from the spectra recorded during the Palestine, Texas, balloon flight on May 18, 1976. Error bars are not shown in the figure but are discussed in the text.

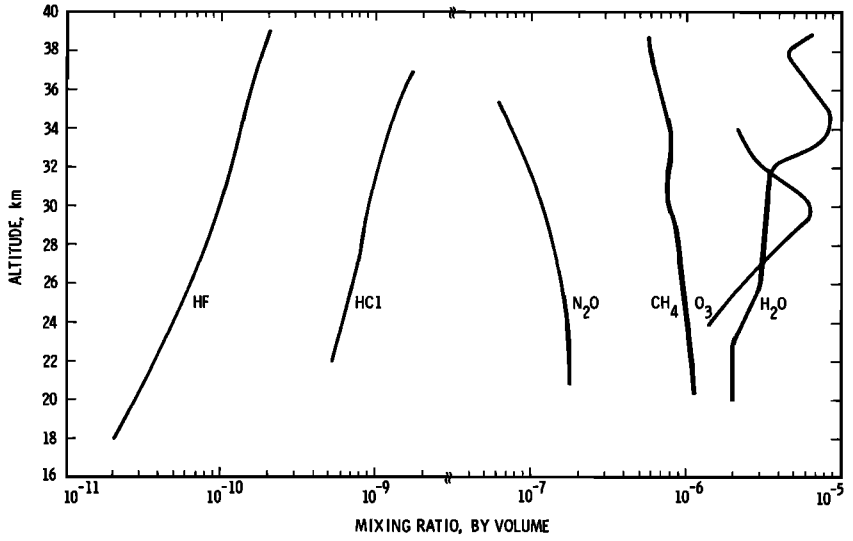

Fig. 2. Volume mixing ratios as a function of altitude for the minor and trace species covered during the Broken Hill, Australia, flight on March 23, 1977. Error bars are not shown in the figure but are discussed in the text.

text with the other minor and trace species included in the measurements.

Water Vapor

One of the more surprising results is the unexpectedly large values for the volume mixing ratio of water vapor found at the higher altitudes in both flights. For the Texas profile in Figure 1 the water vapor increases from 5 ppmv in the lower stratosphere to a maximum of 8.7 ppmv at 35 km. Figure 2 indicates the Australian profile increases with altitude from 2 ppmv to a maximum of 8.3 ppmv at 34 km. The estimated error for both profiles is ±20% at all altitudes. Had the analysis of the spectra for the other relatively well-known gases (for example, CO_2, CH_4) yielded results at significant variance from the currently accepted values, the high water vapor values would have been suspect. Even so, the intrinsic line parameters from *Toth et al.* [1973] for the 12 lines chosen for inclusion in the analysis of both data sets were carefully checked and the stratospheric spectra themselves subjected to independent analysis by several of our colleagues. We have been unable to find any source of systematic or experimental error to account for the large increase in the H_2O volume mixing ratio with altitude illustrated in Figures 1 and 2. It should be added that these analyses have included investigation of the growth of the water vapor features with respect to both line strength and line-of-sight air mass in an attempt to search for any residual absorption of solar origin or from unidentified features in the telluric spectrum. Contamination from either of the latter sources could be manifested as a profile of increasing concentration with height; no such blending interference of any significance could be found.

In addition to the potential sources of error mentioned above, balloon-borne measurements of stratospheric water vapor, and especially those that indicate an increase in mixing ratio with altitude, have traditionally been subject to suspicion on the grounds of the potential presence of outgassed water surrounding the balloon and the instrument gondola. There are several arguments against this being the case in the present instance, the strongest of which is directly supported by the same data used to rule out solar line contamination. If the balloon and gondola were surrounded by a sphere of outgassed water vapor, the contribution from such a source of contamination to the equivalent width of the lines being analyzed would be reasonably constant; that is, they would produce an effect on the growth of lines with air mass spectroscopically indistinguishable from solar line contamination (see discussion on CO below). In the case of the H_2O lines, however, there is no significant absorption present at the relevant frequencies in the spectra recorded before sunset at the higher elevation angles, and we conclude that the measurements are not contaminated by water vapor in the near vicinity of the balloon. The evidence supporting both of the above arguments is contained in the spectra shown in Figure 5.

Previous measurements of the water vapor distribution in the stratosphere have been summarized in a critical review by *Harries* [1976]. With the exception of the infrared measurements of *Chaloner et al.* [1975], the present results do not agree in a quantitative sense with any of the results reviewed by Harries nor with the mean mid-latitude mixing ratio which Harries derives from a subset of the reviewed data. The agreement between these results and those of *Chaloner et al.* [1975] is well within the estimated errors of the respective measurements, although the concentration profile derived from the latter results continues to increase with altitude above 35 km. More recent in situ measurements by *Kley et al.* [1979] at northern mid-latitudes are in excellent agreement with those shown here. Global water vapor measurements are currently being made by the LIMS instrument on Nimbus G, and preliminary analyses of the data have suggested the same trend toward higher mixing ratios in the upper stratosphere and overall profiles which are also in general agreement with the H_2O profiles in Figures 1 and 2 [J. Russell, private communication, 1979].

The present results clearly suggest a significant source of water vapor in the stratosphere. The obvious photochemical source, oxidation of methane, is qualitatively consistent with the CH_4 and H_2O profiles, but this can only account (under equilibrium conditions) for a maximum increase of ~1.4 ppmv of H_2O to match the observed CH_4 depletion at the highest altitude (see later); the observed increase exceeds this value, especially at localized altitudes. A possible explanation for this 'discrepancy' could be the injection of substantial masses of

TABLE 2. Volume Mixing Ratios as a Function of Altitude for the Minor and Trace Species Derived From the Spectra Recorded During Both Balloon Flights

Altitude, km	Pressure, atmosphere	Temperature	O_3, × 10^6		H_2O, × 10^6		CH_4, × 10^6		N_2O, × 10^7		HCl, × 10^9		CO, × 10^8,	HF, × 10^{10},
			30°N	30°S	30°N	30°S	30°N	30°S	30°N	30°S	30°N	30°S	30°N	30°S
18	0.0743	216.5												0.22
19	0.0640	217.5												0.26
20	0.0545	218.5				2.0		1.12						0.30
21	0.0458	219.5				2.0		1.10		1.80				0.35
22	0.0400	221.0	1.9		5.0	2.0	1.3	1.08	1.85	1.75	0.62	0.54	1.0	0.40
23	0.0345	222.5	2.0		5.0	2.2	1.05	1.05	1.8	1.70	0.64	0.58	1.0	0.45
24	0.0295	223.5	2.2	1.6	5.0	2.5	0.95	1.00	1.7	1.65	0.68	0.63	1.0	0.52
25	0.0253	225.2	2.6	2.0	5.0	2.9	0.92	0.98	1.6	1.60	0.71	0.68	1.0	0.59
26	0.0219	227.2	3.0	2.6	5.0	3.0	0.90	0.95	1.5	1.50	0.75	0.73	1.0	0.66
27	0.0188	229.2	3.5	3.4	5.0	3.1	0.87	0.91	1.4	1.4	0.78	0.78	1.0	0.74
28	0.0163	231.0	4.3	4.5	5.5	3.2	0.83	0.85	1.3	1.3	0.82	0.82	1.0	0.84
29	0.0141	233.0	5.4	6.2	6.8	3.3	0.80	0.81	1.2	1.2	0.87	0.87	1.0	0.91
30	0.0122	235.0	6.8	5.7	7.0	3.4	0.76	0.76	1.1	1.1	0.92	0.92	1.0	1.00
31	0.0106	237.2	7.7	3.9	7.0	3.5	0.71	0.77	1.0	1.0	0.97	0.97		1.07
32	0.0092	239.5	7.7	2.7	6.8	4.5	0.66	0.79	0.90	0.90	1.05	1.05		1.17
33	0.0080	241.7	7.0	2.3	7.0	7.3	0.66	0.80	0.75	0.79	1.13	1.13		1.23
34	0.0070	243.7	5.6		8.3	8.3	0.68	0.75	0.60	0.68	1.23	1.23		1.32
35	0.0060	246.2	3.8		8.7	7.3	0.60	0.70	0.40	0.60	1.38	1.38		1.45
36	0.0053	249.0			6.6	6.0	0.50	0.65			1.55	1.55		1.60
37	0.0046	251.5			5.0	4.8	0.45	0.60			1.70	1.70		1.75
38	0.0040	254.0				5.0		0.57						1.85
39	0.0035	256.7				6.0		0.57						2.05
40	0.0031	259.2												

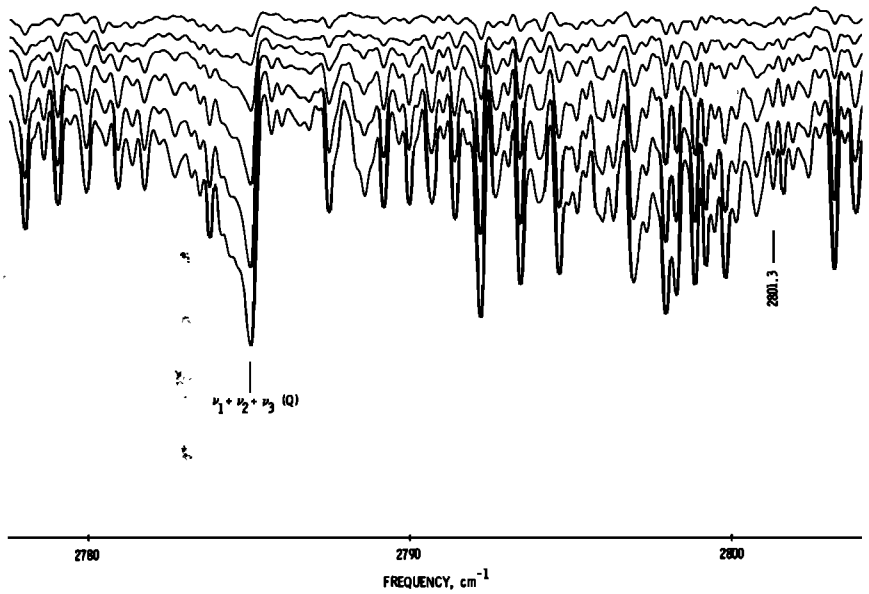

Fig. 3. Excerpts from the Texas spectra showing portions of the $\nu_1 + \nu_2 + \nu_3$ band of O_3 from which the northern ozone profile was derived. The vertical line marks the feature (consisting of a group of O_3 lines), which was used in the data analysis. In this figure and in all subsequent features of a similar nature, the individual spectra have been offset for clarity.

water ice by penetration of thunderstorms through the tropical tropopause. The strong dependence of saturation vapor pressure on temperature would allow reevaporation from the solid phase in the warmer regions of the stratosphere at 30–40 km altitude, where the capacity at saturation far exceeds the present measured values. For example, for a stratospheric temperature of 226 K at 30 km (U.S. Standard Atmosphere, 1972) the upper limit to the volume mixing ratio for water vapor is 10^{-3}, or more than 2 orders of magnitude higher than the measured concentrations. From this point of view it is perhaps somewhat surprising that the transport of H_2O in the solid phase has not been given more consideration in the past. The slow equilibration by diffusion of the injected water could well cause anomalously high water vapor concentrations over large areas which would have a significant impact on the concentrations of hydroxyl radicals.

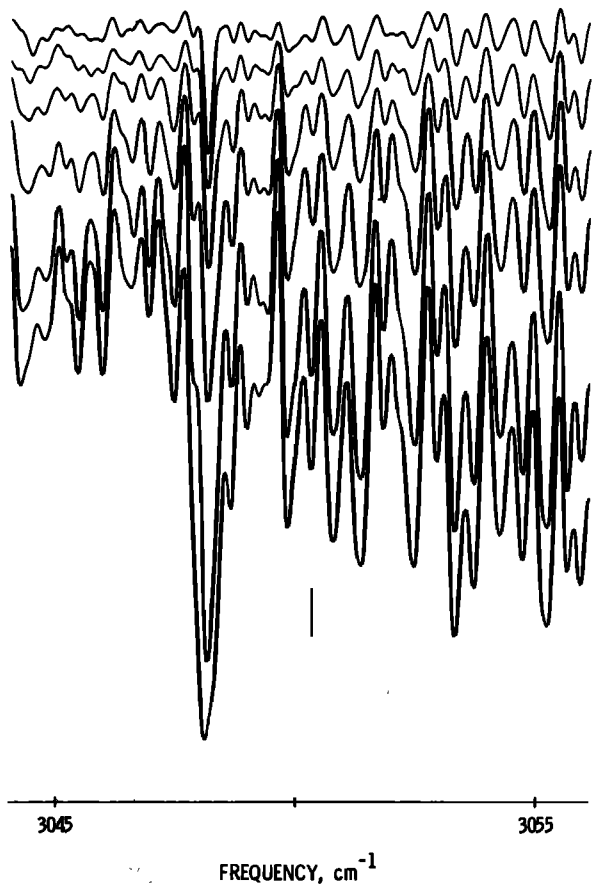

Fig. 4. Excerpts from the Australian spectra showing portions of the $3\nu_3$ O_3 band used to derive the Australian profile. The vertical line in the figure indicates the rotational features which were used for the analysis.

Nitrous Oxide

As Table 1 indicates, several N_2O vibration-rotation bands occur within the region covered by the spectra. These include a large number of unblended lines whose molecular parameters have now been well established from laboratory measurements; thus the N_2O profile can be derived from the spectra with an accuracy approaching that obtainable for CO_2 at the lower altitudes (±10%) but with greater uncertainty at highest altitudes (±30%). Except for differences at the altitude extremes, the profiles for the northern and southern hemisphere are very similar, showing a rapid decrease in volume concentration with increasing altitude (see Table 2).

Several other investigators have measured N_2O concentrations in the lower stratosphere by both spectroscopic and in situ techniques, and, whereas the results from the earlier work showed values ranging from 100–320 ppb at the tropopause, the more recent measurements have converged toward a value closer to 300 ppb in this region. With regard to the variation in the mixing ratio with height, the relevant results for comparison with the present work are the recently published work of *Schmeltekopf et al.* [1977] and the earlier measurements of *Ehhalt et al.* [1975]. Both of these groups used in situ techniques; the *Ehhalt et al.* [1975] results were consistent with the relevant *Schmeltekopf et al.* [1977] values, the latter revealing a considerable variability with location, especially at the higher altitudes (i.e., above 20 km). The present results dem-

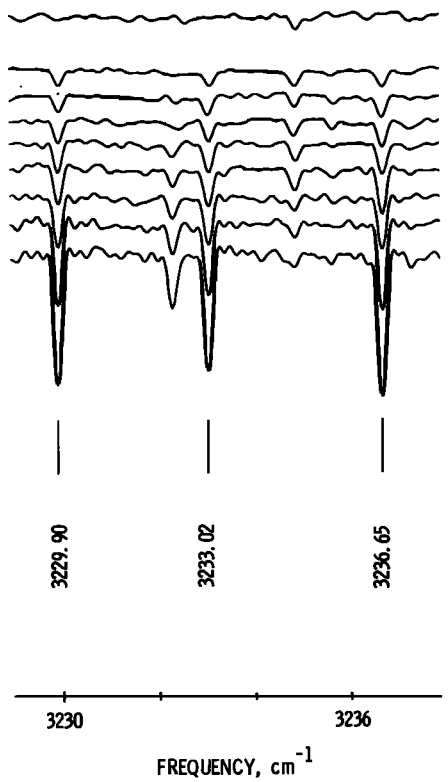

Fig. 5. Portions of several of the (Australian) spectra showing three of the H_2O lines which were used to derive the water vapor profile shown in Figure 2. These same lines were present in the Texas spectra and were used to derive the H_2O profile shown in Figure 1. The uppermost trace in the figure is from a spectrum recorded at a high (>0) solar elevation angle which demonstrates the lack of residual absorption by solar lines or outgassed water vapor surrounding the balloon and gondola.

onstrate the same rapid decrease of concentration with altitude obtained by the in situ measurements and are in close agreement with the *Schmeltekopf et al.* [1977] values for northern mid-latitudes, extending those results to higher altitudes. Schmeltekopf and his co-workers also found the N_2O concentration in the troposphere to be remarkably constant for all latitudes at 320 ± 40 ppbv, and measurements made from the ground prior to the present flights are also in good agreement with their value for the total tropospheric burden (320 ± 30 ppbv prior to the Palestine flight and 330 ± 40 ppbv prior to the flight in Australia).

Hydrogen Chloride

The HCl results from the present Palestine flights and a previous flight in 1975 were published earlier in a review of stratospheric HCl measurements [*Raper et al.*, 1977]. The HCl profile from the earlier paper is shown in context with the other measured gases in Figure 1. The principal features used for the analysis were the P2, R1, and R2 rotational lines of the 1–0 transition of $H^{35}Cl$; the relevant molecular data were taken from *Toth et al.* [1970]. The actual features used are shown for the 1976 flight in Figure 6. Figure 7 shows synthetic spectra in the wavelength regions of these HCl lines, generated with the layered model atmosphere. The smoothed profile from the model which provided the best fit between the synthetic and observed spectra is that shown in Figure 1, which indicates an increase in the vertical mixing ratio of HCl from 0.6 ppbv at 21 km to 1.7 ppbv at 37 km. The established overall accuracy of the measurements is ±30% at the altitude extremes (as a result of the weakness of the features at the upper bound and continuum uncertainties at the lower) and ±20% in the region from 24 to 32 km.

While the three lines shown in Figure 6 were the most useful for the HCl analysis, they were by no means the only HCl features present in the spectra. Although many of the lines are too weak or too severely blended to be seen at our present resolution, in each case where circumstances indicate an HCl feature should be discernable in the spectra, a line is in fact present whose equivalent width is consistent with the profile derived from the more prominent features. Most of the weaker features are seen only at the larger solar depression angles (i.e., at the largest air masses). Figure 8 shows a number of additional HCl lines which appear in the same spectra from which the two lowest traces in Figure 6 were extracted and demonstrates with synthetic spectra that these features are consistent with the profile shown in Figure 1.

The HCl analysis was more difficult with the Australian spectra than was the case with the earlier Texas data, because the HCl features were close to the long wavelength cutoff of the order isolation filter through which they were recorded. The frequency of the P2 line, used in the analysis of the Palestine data, was not covered by the filter, and the frequencies of the R1 and R2 HCl lines, which were those used in the Australian data analysis, fall within a region where the optical filter transmits only about 30% of the incoming radiation, as

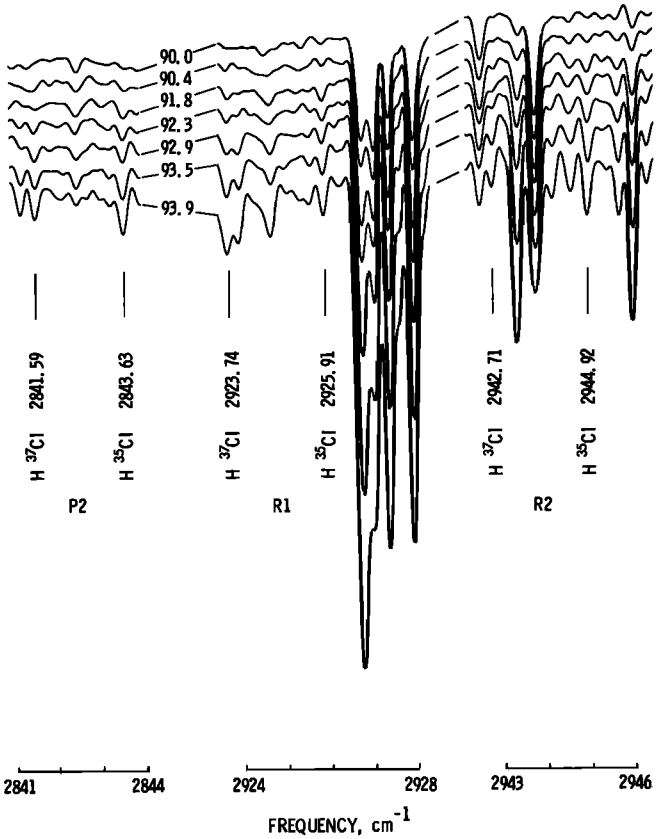

Fig. 6. Portions of the set of stratospheric spectra covering the P2, R1, and R2 lines of the 1-0 HCl transition obtained during the Texas balloon flight. The line positions for both chlorine isotopes are shown in the figure; the three $H^{37}Cl$ lines are blended with features of other atmospheric gases (principally methane) and were not used in the quantitative analysis. The angles shown are the (astronomical) solar zenith angles at which the spectra were recorded.

Fig. 7. Synthetic spectra over the P2, R1, and R2 region of HCl, generated to match the spectra shown in Figure 6 (see text).

compared to about 80% for the filter used during the northern hemisphere flight. Thus the error limits are considerably larger in the Australian measurements, being estimated at ±50% at the altitude extremes and ±30% in the mid-stratosphere. Within these limits the profile of concentration shown in Figure 2 is generally the same as that measured at northern mid-latitudes.

A comparison between the present results and those of other investigators is shown in Figure 9. There is some general agreement between our results and the spectroscopic results of *Ackerman et al.* [1976] and *Williams et al.* [1976] but rather poor agreement between the present profile and that obtained by *Eyre and Roscoe* [1977], using a pressure modulated radiometer (PMR). Since PMR measurements do not retrieve data in a form which can be directly compared to spectral plots, it is difficult to assess the relative reliability of the two sets of measurements. The theoretical advantage of the PMR technique lies in its ability to utilize all of the spectroscopic information in its bandpass attributable to the species being measured; the primary disadvantage lies in the fact that no spectral information is retrieved, and hence the results are critically dependent on the assumed distributions of potentially interfering species. In the present case the primary source of interference is CH_4, the ν_3 band of which dominates the spectral region encompassing the 1-0 transition of HCl. It is critical to the analysis of the PMR data that both an accurate distribution and reliable spectroscopic data for CH_4 be used in the atmospheric model, and it is only recently that either of these has become available. It would perhaps be useful to reanalyze the PMR data using the recently published molecular data of *Toth et al.* [1977] and the CH_4 profile shown in Figure 1.

The acid chloride data shown in Figure 9 are the average of four seasonal profiles measured in 1976 by using in situ techniques [*Lazrus et al.*, 1977]. The sampling method used is presumably sensitive to all inorganic chlorides and, in the absence of local variations, should yield results equal to or greater than those obtained from spectroscopic measurements. Although the in situ results are in reasonable agreement with all of the measurements made in the 15- to 25-km region of the stratosphere, they are consistently lower than those obtained spectroscopically above 25 km. While the two techniques differ considerably and must therefore be compared with caution, the magnitude of the discrepancy and its persistence preclude the possibility of attributing it solely to the experimental methods themselves, but strongly suggests a significant systematic error in one of the techniques. Until a satisfactory explanation for the discrepancy is forthcoming, it must be viewed as an additional uncertainty in all of the HCl values for the upper atmosphere.

Hydrogen Fluoride

One of the primary objectives of the Australian flight was to obtain the vertical concentration profile of HF, the presence of which was confirmed earlier by *Zander et al.* [1977]. This molecule is the primary sink for fluorine in the stratosphere, and in view of the fact that no major sources of stratospheric fluorine other than the CFM's have been identified, it can be related more straightforwardly to them than can the HCl, for which other known sources exist. Furthermore, the ratio of

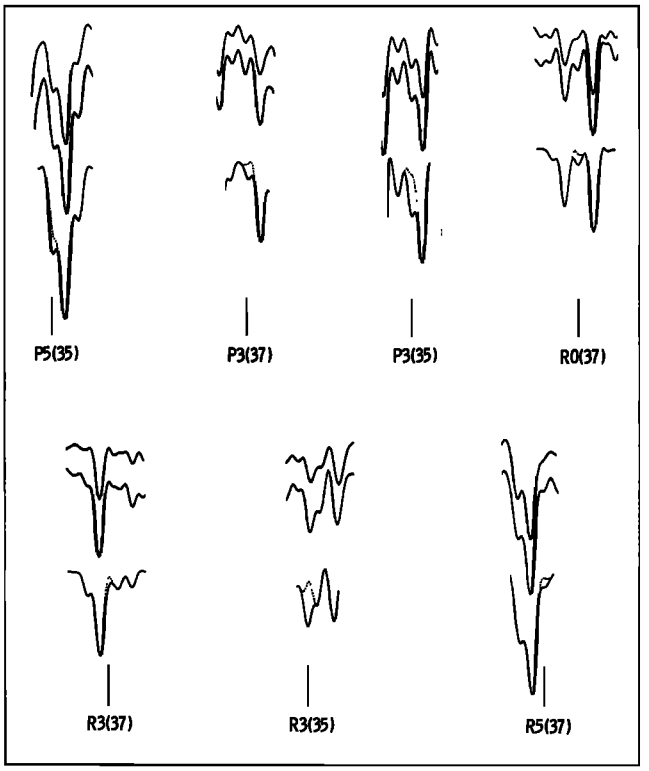

Fig. 8. Portions of the same spectra from which the two lowermost traces in Figure 6 were extracted in the regions where a number of weak and blended HCl features absorb. The third (bottom) trace in each case is a synthetic spectrum of the region using the same HCl distribution used to generate the spectra in Figure 7. The dashed lines in these traces represent the same region without HCl.

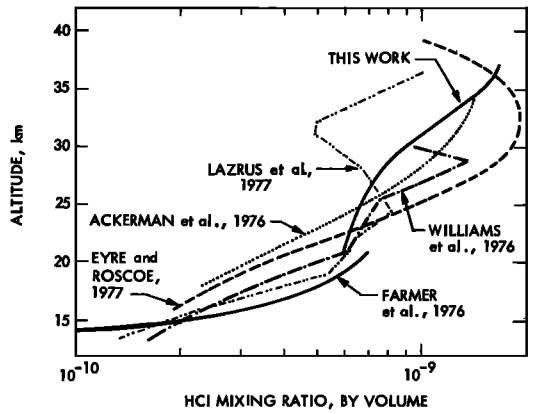

Fig. 9. Comparison of the HCl results reported here with those derived from other measurements (discussed in text).

HF to HCl as a function of altitude in the stratosphere is important in that it provides a check on the fate of the dissociation products. Since the 1–0 fundamental transitions for both gases were covered in the Australian flight, it was possible to obtain this ratio directly from the spectra by ratioing

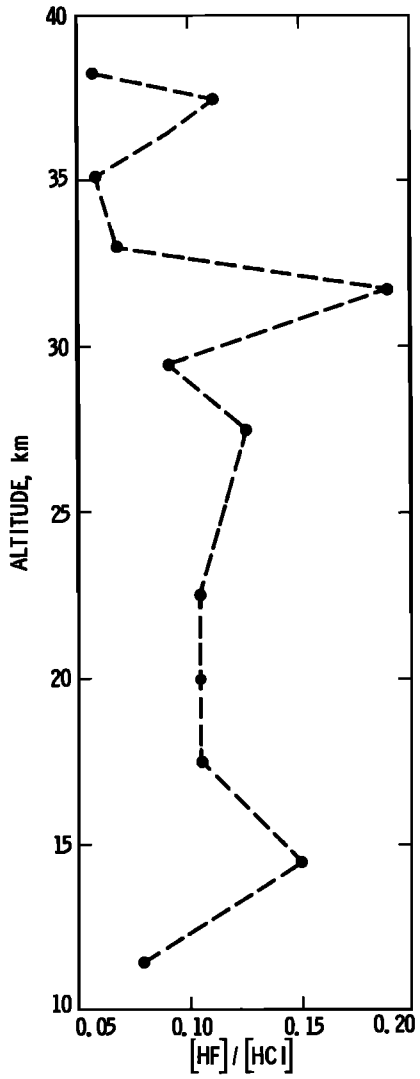

Fig. 10. Ratio of the molecular density of HF to HCl as a function of altitude in the stratosphere inferred from the Australian spectra.

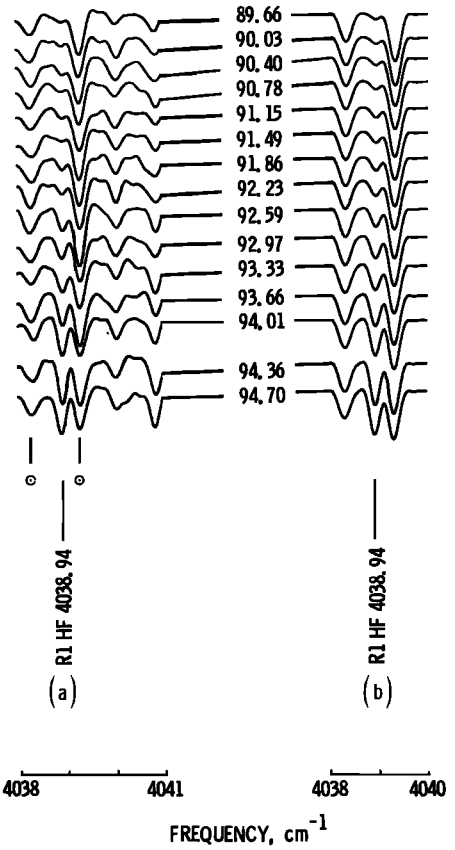

Fig. 11. (*a*) Excerpts in the region of the R1 line of the 1-0 HF transition from the set of Australian spectra recorded at sunset on March 23, 1977, near Broken Hill. The angles shown are the (astronomical) zenith angles. (*b*) Synthetic spectra generated to match the spectra shown in (*a*) (see text).

the apparent equivalent widths of the R1 lines for each gas by using the molecular parameters referenced above for HCl and those of *Goldman et al.* [1974] for HF. Ratioing the line pairs was greatly facilitated by the fortuitous fact that the lines were nearly equal in size, eliminating any curve of growth effects. The HF/HCl ratio thus obtained was published earlier, [*Farmer and Raper*, 1977] and is reproduced in Figure 10. The relatively large errors associated with the ratio (±30% in the midstratosphere and ±50% at the altitude extremes) are primarily due to uncertainties in the Australian HCl profile.

The R1 line of the HF 1-0 transition used to obtain the HF/HCl ratio was also used to derive its vertical profile of concentration, since this is the only HF feature free from blending at our present resolution. The set of R1 lines from the Australian spectra are shown in Figure 11, together with the corresponding synthetic spectra generated with the liquid model atmosphere. The HF profile used in the model atmosphere which produced the best match between the real and synthetic features is that shown in Figure 2. As the figure indicates, the HF volume mixing ratio increases with altitude in a manner generally similar to the HCl profile, from a value of 2.2×10^{-11} at 18 km to 2.1×10^{-10} at 38 km. The estimated uncertainty in these values is ±20%.

The discussion of HF in the earlier HF/HCl ratio publication [*Farmer and Raper*, 1977], which compared our results with those of *Zander et al.* [1977] and *Mroz et al.* [1977], was provisional, relying on the assumption that the Australian HCl profile would not differ materially from our earlier Pales-

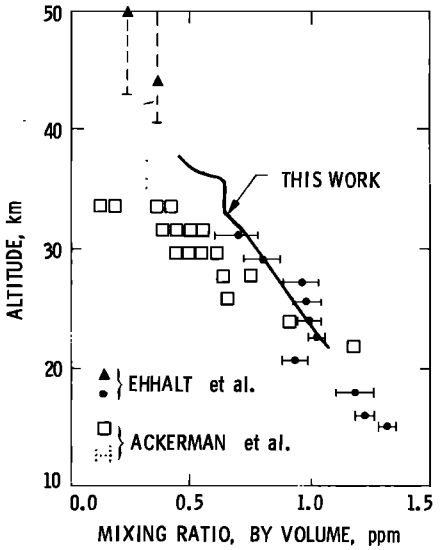

Fig. 12. A comparison of the CH_4 results shown in Figures 1 and 2 with those of other investigators (discussed in text).

tine, Texas, results [*Raper et al.*, 1977] and thus that the HF profile could be inferred from the ratio. Since this assumption proved to be essentially correct, the actual profile shown here is equivalent to the one inferred from the HF/HCl ratio, and the earlier comparisons are still valid. If it is assumed that the only fluoride collected by the in situ sampling technique of *Mroz et al.* [1977] is HF, there is very good agreement between the present results and those from the in situ measurements with regard to the total amount of HF above 27 km. Although the profiles are different, both sets of data indicate that HF constitutes $\sim 1.2 \times 10^{-10}$ of the total volume of air above that altitude. *Zander et al.* [1977] did not measure the HF profile, but their value for the total burden above 27 km, expressed as above, was 3.6×10^{-10}, a factor of 3 greater than the present results. It should be pointed out here that *Derwent and Eggleton* [1978], in their publication describing the Harwell model atmosphere, misinterpreted the *Zander et al.* [1977] result when comparing it with their model. They refer to it as the volume mixing ratio at 27 km, stating that it agrees well with their modeled result of 3.5×10^{-10}. The 3.6×10^{-10} value does not represent the mixing ratio at 27 km, however, but rather the volume ratio of total HF to total air above 27 km. It is the modeled value of this quantity that should be compared with the measured results.

Irrespective of the degree of agreement with the models, it is clear that the two spectroscopic results are in disagreement to an extent which is well outside the combined estimated errors. In view of the importance of the HF concentration profile to the modeling community, this discrepancy needs to be resolved, and toward this end additional measurements of HF are planned to be made by both groups.

Methane

Methane absorption features associated with numerous vibrational transitions are prevalent over most of the wavelength region covered in the two balloon flights, the most prominent being those of the ν_3 transition centered at 3.31 μm. Spectroscopically, methane is the most complex of all the minor atmospheric constituents, and as a result reliable data with regard to its spectroscopic parameters (particularly at stratospheric temperatures) have been very limited. The recent publication of *Toth et al.* [1977] concerning methane in this region has provided much more reliable data for the molecular parameters than were previously available in the literature, and these values were used in the inversion of several unblended lines and manifolds to derive the profiles for CH_4 shown in Figures 1 and 2. The Palestine data are consistent with a methane profile having a mixing ratio of 1.3×10^{-6} at 21 km, decreasing to 4.5×10^{-7} at 37 km. The accuracy of these values is estimated to be ±15% and ±25%, respectively. Like N_2O, the Australian CH_4 in comparison with the Palestine CH_4 shows slightly smaller concentrations in the lower stratosphere but falls off less rapidly at the upper bound of the measurements.

The only previous results above 30 km are those of *Ackerman et al.* [1977], derived from infrared spectra covering the 2916–2970 wave number region, and those of *Ehhalt et al.* [1975], using an in situ sampling technique. The present spectroscopic results are higher than those of *Ackerman et al.* [1977] but are in good agreement with those obtained by the earlier in situ sampling measurements. More recent measure-

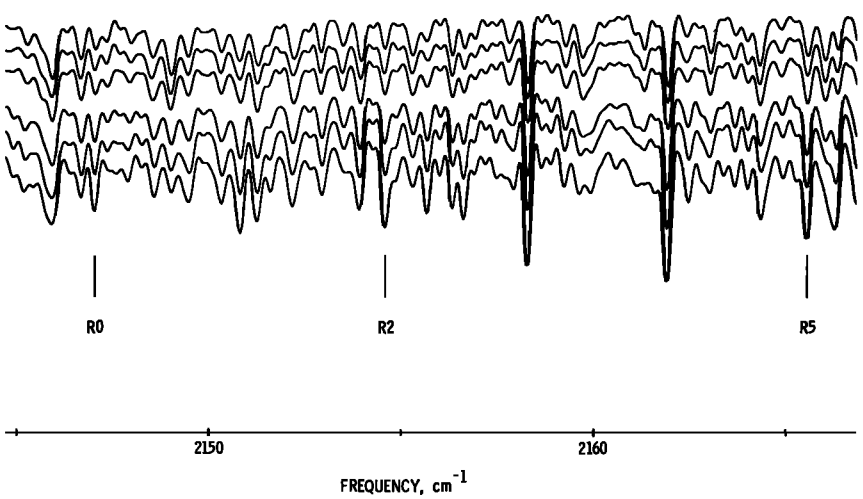

Fig. 13. Portions of several of the Texas spectra in the region of the 1-0 CO transition. The features marked with vertical bars were those used for the CO analysis. The three upper traces in the figure were taken from spectra at high (>0) solar elevation angles and represent the contribution to the equivalent widths of the CO lines due to solar CO.

ments by this group, however, have yielded results in the 20- to 31-km region of the stratosphere, which are lower than those obtained previously [P. Crutzen, private communication, 1979], although still somewhat higher than those of *Ackerman et al.* [1977].

A comparison of the relevant CH_4 results is shown in Figure 12. Although it cannot be ruled out entirely, it would appear unlikely that the rather large variation in stratospheric CH_4 implied by the various measurements is real. In view of the importance of CH_4 as a source of stratospheric water vapor and hence OH and HO_2 radicals, there is clearly a need for additional measurements of its vertical abundance.

Carbon Monoxide

As was stated earlier, the only CO features of telluric origin in either set of spectra were those of the 1-0 fundamental transition centered at 2143 cm^{-1} recorded during the Palestine flight. Portions of several of the spectra in this region are shown in Figure 13. The analysis of the CO features is complicated by virtue of the fact that a significant fraction of the equivalent width of each line is due to CO absorption in the solar photosphere. In those spectra having tangent heights greater than about 30 km, the CO features are totally dominated by the solar contribution. To analyze these features correctly, it is necessary to take into account the formation of the solar lines at photospheric temperature to define the continuum upon which the stratospheric absorption is superimposed. This can be done straightforwardly, since the constant residual solar lines are clearly discernable in all of the higher elevation spectra (see Figure 13). R0, R2, and R5 were the solar lines used for the analysis. They were assumed to have a pure Doppler profile, formed at 5000 K, and their intensities were adjusted to match the observed spectra at the smallest elevation angles. These features were then held fixed in the model, and the stratospheric CO distribution was iterated to a best fit with the observed spectral lines. The results obtained by using this procedure (shown in Figure 1) are indicative of a constant volume mixing ratio for CO of 1.0×10^{-8} between 21 km and 30 km with uncertainties of $\pm 0.2 \times 10^{-8}$ at the lower altitude and $\pm 0.5 \times 10^{-8}$ at the upper bound.

Atmospheric CO concentrations have been measured previously in the near infrared by *Goldman et al.* [1973] and *Farmer* [1974] which show a decrease in the CO mixing ratios in the lower stratosphere which is consistent with the values shown here for higher altitudes. In situ measurements have been made by *Seiler and Warneck* [1972] and *Ehhalt et al.* [1975] in the lower stratosphere, which are in good agreement with the infrared results. The values for the CO mixing ratio reported by *Ehhalt et al.* [1975] for the middle stratosphere were considerably higher than those shown in Figure 1 and indicated an increase in the CO mixing ratio above 25 km.

Carbon Dioxide

The ν_3 fundamental band and numerous combination bands of CO_2 occur at frequencies within the range covered by the observations, as is indicated in Table 1. The very large range of intrinsic line strengths and temperature dependences thus available provides a powerful test of the observational geometries associated with the individual measurements and of the atmospheric model adopted for the analysis of the other molecular species. By simultaneous measurements of several CO_2 lines in both data sets, a constant mixing ratio of $3.3 \pm 0.3 \times 10^{-4}$ was derived in the 21- to 39-km altitude range of the stratosphere. The accuracy of the CO_2 measurements is higher than that quoted for most of the other species because of the large number of accessible lines of optimum intensity in each observation which can be included in the analysis. The resultant accuracy thus approaches that obtained by using in situ techniques. An example of the close agreement obtained between the observed and synthetically generated CO_2 spectra for the temperature sensitive high J region of the ν_3 band from the Palestine observations is shown in Figure 14. The importance of the CO_2 result in the present context is that it minimizes the systematic error associated with errors in the atmospheric model and the observational geometry and thus improves the accuracy of the absolute values derived for the other species.

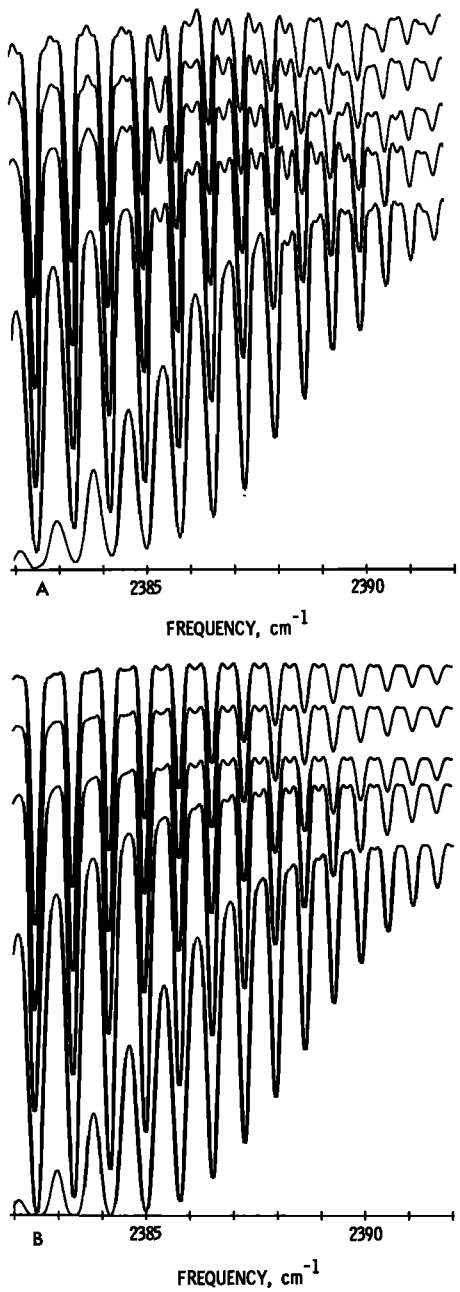

Fig. 14. The high J region (R52–R80) of the ν_3 CO_2 transition (*a*) from the Texas spectra and (*b*) from synthetic spectra generated with the model atmosphere used for the analysis of the data, with a constant mixing ratio of 3.3×10^{-4} for CO_2.

CONCLUSIONS

Two composite sets of vertical profiles of concentration for a number of the minor and trace molecular species in the 20- to 40-km altitude range have been derived from the observed spectra. The usefulness of the results lies in the fact that the systematic errors in the present approach are significantly reduced by virtue of the fact that the measurements are made simultaneously; the relative accuracy is therefore high, since geometric factors are common to the analyses of all species and should be limited solely by the accuracy of the laboratory data for transition strengths and half widths and their temperature dependences. The absolute accuracy can most usefully be judged from comparison of the results obtained for a fairly well-understood species, such as CO_2. The results should thus provide a useful constraint against which the predictions related to relevant subsets of species in current photochemical models can be tested. As a general conclusion, it appears that many of the vertical profiles for the species are in accord with those from previous measurements and the model predictions. The CO results reported here, although considerably lower than those measurements which were published previously, are in excellent agreement with present model predictions. Water vapor, on the other hand, shows considerably larger abundances at the higher altitudes than the majority of the previously published profiles, exceeding in fact the increase with height predicted on the basis of methane oxidation alone. In the case of HF the present measurements are at variance with model predictions as well as the other published spectroscopic results, and more measurements of the concentration profile for this gas are clearly needed.

Acknowledgments. The authors would like to express their gratitude to H. Geise, R. Killian, R. Perrin, J. Riccio, P. Schaper, and R. Wilson for their engineering and technical assistance in integrating the JPL instrument into the balloon gondola and conducting the Palestine and Broken Hill flights. A large share of the credit for the success of the flights must also go to the NSF NCAR personnel who staff the Palestine facility, for whose advice and professional services the authors are equally grateful. For the Australian flight we are particularly indebted to R. A. Leslie of the Australian Department of Science, who coordinated the Australian efforts, to P. Oats, who directed the launch, and to the able Australian launch crew for their patience and persistence during the launch and recovery operations. Selected spectra from the two data sets which were obtained during the Texas and Australia flights are currently being prepared for publication as a stratospheric atlas, a copy of which will be made available to any potential user. In the interim, relevant portions of the data will be made readily available to any interested scientist. This paper is JPL Atmospheres Publication Number 979-9 and presents the results of one phase of the research carried out at the Jet Propulsion Laboratory, California Institute of Technology, under contract NAS 7-100, sponsored by the Upper Atmospheric Research Office, Office of Space and Terrestrial Applications, National Aeronautics and Space Administration.

REFERENCES

Ackerman, M., D. Frimout, A. Girard, M. Gottignies, and C. Muller, Stratospheric HCl from infrared spectra, *Geophys. Res. Lett., 3,* 81–83, 1976.

Ackerman, M., D. Frimout, and C. Muller, Stratospheric CH_4, HCl, and ClO and the chlorine-ozone cycle, *Nature, 269,* 226–227, 1977.

Chaloner, C. P., J. R. Drummond, R. F. Jarnot, J. T. Houghton, and H. K. Roscoe, Stratospheric measurements of H_2O, NO, and NO_2, *Nature, 258,* 696–697, 1975.

Derwent, R. G., and A. E. G. Eggleton, Ozone depletion estimates for global halocarbon and fertilizer usage employing one-dimensional modeling techniques, *Rep. AERE-R 9112,* AERE Harwell, Harwell, England, August, 1978.

Ehhalt, D. H., L. E. Heidt, R. H. Lueb, and W. Pollock, The vertical distribution of trace gases in the stratosphere, *Pure Appl. Geophys., 113,* 389–402, 1975.

Eyre, J. R., and H. K. Roscoe, Radiometric measurements of HCl, *Nature, 226,* 243–244, 1977.

Farmer, C. B., Infrared measurements of stratospheric composition, *Can. J. Chem., 52,* 1544–1559, 1974.

Farmer, C. B., and O. F. Raper, The HF:HCl ratio in the 14- to 38-km region of the stratosphere, *Geophys. Res. Lett., 4,* 527–529, 1977.

Farmer, C. B., O. F. Raper, and R. H. Norton, Spectroscopic detection and vertical distribution of HCl in the troposphere and stratosphere, *Geophys. Res. Lett., 3,* 13–16, 1976.

Goldman, A., D. G. Murcray, F. H. Murcray, W. J. Williams, J. N. Brooks, and C. M. Bradford, Vertical distribution of CO in the atmosphere, *J Geophys. Res., 78,* 5273–5283, 1973.

Goldman, A., S. C. Schmidt, J. R. Riter, and R. M. Blunt, Infrared spectral radiance of hot HF and DF in the $v = 1$ bands region as seen through an atmospheric path, *J. Quant. Spectrosc. Radiat. Transfer, 14,* 299–307, 1974.

Harries, J. E., The distribution of water vapor in the stratosphere, *Rev. Geophys. Space Phys., 14,* 565–575, 1976.

Kley, D., E. J. Stone, W. R. Henderson, J. W. Drummond, W. J. Harrop, A. L. Schmeltekopf, and T. L. Thompson, In situ measurements of the mixing ratio of water vapor in the stratosphere, *J. Atm. Sci.,* in press, 1979.

Lazrus, A. L., B. W. Sandrud, J. Greenberg, J. Bonelli, E. Mroz, and W. A. Sedlacek, Mid-latitude seasonal measurements of stratospheric acid chlorine vapor, *Geophys. Res. Lett., 4,* 587–589, 1977.

McClatchey, R. A., W. S. Benedict, S. A. Clough, E. D. Burch, R. F. Calfee, K. Fox, L. S. Rothman, and J. S. Garing, AFCRL atmospheric absorption line parameters compilation, *AFCRL-TR-0096, Environ. Res. Pap. 434,* Air Force Cambridge Res. Lab., Bedford, Mass., 1973.

Mroz, E. J., A. L. Lazrus, and J. Bonelli, Direct measurements of stratospheric fluoride, *Geophys. Res. Lett., 4,* 149–150, 1977.

Raper, O. F., C. B. Farmer, R. A. Toth, and B. D. Robbins, The vertical distribution of HCl in the stratosphere, *Geophys. Res. Lett., 4,* 531–534, 1977.

Schindler, R. A., A small, high speed interferometer for aircraft, balloon, and spacecraft applications, *Appl. Opt., 9,* 301–306, 1970.

Schmeltekopf, A. L., D. L. Albritton, P. J. Crutzen, P. D. Goldman, W. J. Harrop, W. R. Henderson, J. R. McAfee, M. McFarland, H. I. Schiff, T. L. Thompson, D. J. Hoffman, and N. T. Kjome, Stratospheric nitrous oxide profiles at various latitudes, *J. Atmos. Sci., 34,* 729–736, 1977.

Seiler, W., and P. Warneck, Decrease of carbon monoxide mixing ratio at the tropopause, *J. Geophys. Res., 77,* 3204–3214, 1972.

Toth, R. A., Strengths and air-broadened widths of H_2O lines in the 2950–3400 cm^{-1} region, *J. Quant. Spectrosc. Radiat. Transfer, 13,* 1127–1142, 1973.

Toth, R. A., R. H. Hunt, and E. K. Plyler, Line strengths, line widths and dipole moment function for HCl, *J. Mol. Spectrosc., 35,* 110, 1970.

Toth, R. A., L. R. Brown and R. H. Hunt, Line positions and strengths of methane in the 2862 to 3000 cm^{-1} region, *J. Mol. Spectrosc., 67,* 1–33, 1977.

Williams, W. J., J. J. Kosters, A. Goldman, and D. G. Murcray, Measurement of the stratospheric mixing ratio of HCl using infrared absorption technique, *Geophys. Res. Lett., 3,* 383–385, 1976.

Zander, R., G. Roland, and L. Delbouille, Confirming the presence of hydrofluoric acid in the upper stratosphere, *Geophys. Res. Lett., 4,* 117–120, 1977.

(Received June 29, 1979;
revised November 1, 1979;
accepted November 9, 1979.)